Relativistic propagators for $\pi\pi$ resonances and the NN interaction

M. L. Nack,* T. Ueda,† and A. E. S. Green
Department of Physics and Astronomy, University of Florida, Gainesville, Florida 32601
(Received 29 March 1973; revised manuscript received 19 April 1974)

A relativistic resonance propagator is presented whose form is guided by an approximation to the full S matrix, utilizing K-matrix unitarization of the lowest-order quantum-field-theory perturbation term. This propagator is designed to fit the full S matrix and therefore the corresponding phase-shift data, and to also satisfy a threshold scattering-length relationship. The formalism is generalized to include the propagation of a system of resonances on an individual phase shift, such as occurs on the $\pi\pi$ S wave. A dispersion relation is then used to obtain the corresponding spectral function (or mass-squared distribution). The influence of inelasticity is considered. This model is fitted to several $\pi\pi$ S- and P-wave phase-shift solutions. The spectral functions so obtained can be used in calculations of the $\pi\pi$-system exchange contributions to the NN interaction. The implications of these spectral functions upon the nonrelativistic configuration-space one-boson exchange potential for the NN interaction as well as upon the corresponding relativistic momentum-space potential for use with the Bethe-Salpeter equation are discussed.

I. INTRODUCTION

In attempting to solve problems in strong interactions, such as the $\pi\pi$ and NN interactions, the Feynman-Dyson (FD) S-matrix expansion of quantum field theory is found to be a good starting point. However, because of strong coupling one usually uses a model based on a truncated version of this expansion. This treatment has been very successful in the one-boson exchange potential (OBEP) models[1,2] for the NN interaction in which the higher-order effects are regarded as being represented by heavy-boson exchange contributions. The truncation usually destroys the unitarity of the model, and one can then choose one of many methods of unitarization (see Sec. II) to obtain a unitary model. The K-matrix unitarization is applied to $\pi\pi$ scattering in this paper, and it has been employed in many applications of strong interactions,[3] including NN calculations by one of the authors (T. Ueda).[1,4] One accomplishment of unitarization procedures is the approximate inclusion of higher-order effects.

Following the recent review by Ueda[5] we describe the scattering of nucleons $NN\to NN$ shown in Fig. 1(a) with initial momenta p_1 and p_2, and final momenta p_1' and p_2', by the Mandelstam variables

$$s=-(p_1+p_2)^2, \tag{1.1}$$

$$t=-(p_1'-p_1)^2, \tag{1.2}$$

$$u=-(p_2'-p_1)^2. \tag{1.3}$$

Here $p^2=\vec{p}^{\,2}-E^2$, and $p^2=-M^2$ on the mass shell of a nucleon with mass M. In the NN center-of-mass (c.m.) frame $t=t(\vec{k})=-\vec{k}^2$, where $\vec{k}^2$ is the squared three-momentum transfer between initial and final nucleons. The s channel ($s\geq 4M^2$, $t\leq 0$, $u\leq 0$) describes $NN\to NN$, and the t channel ($t\geq 4M^2$, $s\leq 0$, $u\leq 0$) describes $N\bar{N}\to N\bar{N}$. For a more detailed discussion of the relationship between $NN\to NN$ and $N\bar{N}\to N\bar{N}$ through crossing symmetry and further references see the review by Ueda,[5] and the work of Wong and others in this field.[6,7]

In Secs. II–V we analyze the t-channel interactions

$$N\bar{N}\to\pi\pi\to B_r\to\pi\pi\to N\bar{N}, \tag{1.4}$$

where B_r is a resonance state of the $\pi\pi$ system, and focus on the physical process $\pi\pi\to B_r\to\pi\pi$, which is shown in Fig. 1(b). The $\pi\pi$ phase shifts describing this process will be denoted by δ_l^I, where I will be suppressed when possible. To be consistent here with other $\pi\pi$ analyses we will let this process be described by the $\pi\pi$ s channel, where now

$$s=(2E_\pi)^2=4(\vec{q}^{\,2}+m_\pi^2)=M_{\pi\pi}^2=m^2\geq 4m_\pi^2 \tag{1.5}$$

in the c.m. frame of the $\pi\pi$ system. Here $E_\pi^2=q^2+m_\pi^2$, where q^2 is the squared three-momentum of a π. We will let $a_r=4m_\pi^2$ be the threshold for producing B_r, with mass parameter $m_r=s_r^{1/2}$ and variable mass $m=M_{\pi\pi}$.

In Sec. VI we assume our analysis in the physical s channel of $\pi\pi\to B_r\to\pi\pi$, where $s\geq a_r$ can be applied as an unphysical (virtual) exchange process in the unphysical t channel of $NN\to NN$ where $t=-k^2\leq 0$. The goal is to obtain the correlated part of the 2π exchange contribution to $NN\to NN$.

There are two separate but related problems in OBEP models of the NN interaction: (a) how to couple B with N at the NNB vertex, and (b) how to propagate B between vertices. These problems are related to whether we just use lowest-order

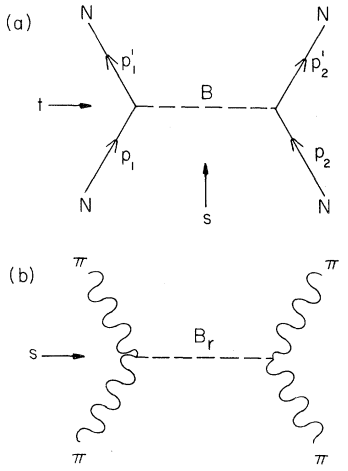

FIG. 1. The lowest-order Feynman diagrams of the (a) *NN* and (b) $\pi\pi$ systems.

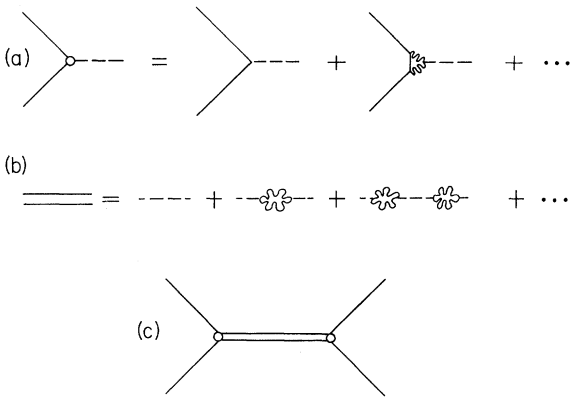

FIG. 2. A Feynman-diagram representation of higher-order perturbation-theory expansions of (a) the *NNB* vertex, and (b) the *B* propagator. The OBEP diagram (c) of the *NN* system including higher-order vertex and propagator effects is also shown.

perturbation theory and treat N and B as elementary point particles, or whether we treat N and B as composite particles with structure and therefore try to include higher-order effects. This is shown by the diagrams of Fig. 2, where Fig. 2(a) represents an expansion of the *NNB* vertex, and Fig. 2(b) represents an expansion of the B propagator. The diagram for an OBEP including both vertex and propagator higher-order effects is shown in Fig. 2(c), where treating N and B as composite particles implies using renormalized fields, masses, and coupling constants. The general *NNB* coupling[8] and the singular part of the B propagator[9] can be expressed by

$$\mathcal{H}_{NNB} = g_{NNB} F(t) \bar{\psi}^N \Gamma_i \psi^N \phi_i^B , \tag{1.6}$$

$$\Delta(t, \Gamma_r) = \int_{-\infty}^{\infty} \rho(t') \Delta(t, t') dt' , \tag{1.7}$$

$$\Delta(t, t') = (t' - t - i0)^{-1} , \tag{1.8}$$

$$\int_{-\infty}^{\infty} \rho(t') dt' = 1 . \tag{1.9}$$

Here $F(t)$ is the *NNB* vertex form factor, and $\rho(t')$ $= \rho(t', t_r, \Gamma_r)$ for variable mass $t' = m'^2$ is the normalized spectral function or invariant-mass-squared distribution peaked about $t' = t_r = m_r^2$, with Γ_r the full width at half height of the distribution at t_r. $\Delta(t, t_r)$ is the lowest-order zero-width part of $\Delta(t, \Gamma_r)$, where $i0$ denotes the limit of $i\epsilon$ as $\epsilon \to 0$. The lowest-order term on the right-hand side of Fig. 2(a) represents $F(t) = 1$, or local coupling between N and B elementary particles, and $\rho(t', t_r)$ $= \delta(t' - t_r)$ treats B as elementary where the first term on the right-hand side of Fig. 2(b) gives the resulting propagator $\Delta(t, t_r)$. In our OBEP at the *NNB* vertex we will use the one-parameter $\frac{1}{2}N$-pole form factor of Ueda and Green[2(b)]:

$$F^{N/2}(t, t_\Lambda) = [t_\Lambda (t_\Lambda - t)^{-1}]^{N/2} = [t_\Lambda \Delta(t, t_\Lambda)]^{N/2} , \tag{1.10}$$

where $t_\Lambda = \Lambda^2$, and $(F^{N/2})^2 = F^N$. This represents the nonlocal coupling on the left-hand side of Fig. 2(a), or higher-order vertex effects; e.g., the t channel of the second term on the right-hand side of Fig. 2(a) represents $N\bar{N} \to \pi\pi \to B_r$. Using F^N is equivalent to using the Nth-order generalized field theory of Green.[2(a), 10] The Fourier transform of $F(t)$ can be viewed as the pion-cloud distribution about N.[2(b)] In this paper we present the details of our four-parameter spectral function $\rho(t', t_r, \Gamma_r, a_r, b_r)$ used to represent the propagator of the composite B_r shown on the left-hand side of Fig. 2(b),[8,11] where $b_r = \Lambda_r^2$ is analogous to a cutoff parameter. All four parameters are obtained from a fit to the $\pi\pi$ phase-shift data.

To obtain our resonance propagators we follow the general analysis of resonances of Jackson,[12] which was later extended by Pišút and Roos[13] (PR) in their study of the ρ meson. We first perform a relativistic phenomenological selection of our amplitude, and note its relationship to the nonrelativistic Breit-Wigner (BW) amplitude following PR. We then relate our amplitude to the lowest-order FD S-matrix expansion term, the Born term, by utilizing K-matrix unitarization. This guides us in our identification of propagators. As Jackson noted, higher-order uncalculable effects can account for the difference between theoretical and empirical resonance shape functions. Therefore the functional form of the lowest-order calculations should only be used as a guide in trying to fit the full S matrix and corresponding phase-shift

data. Our amplitude is generalized to include the propagation of a system of resonances on an individual phase shift, such as occurs on the $\pi\pi$ S wave. A dispersion relation is then used to obtain the corresponding spectral function (or mass-squared distribution) and mass distribution, and the influence of inelasticity is considered.

This model is then fitted to several $\pi\pi$ $S(\delta_0^0)$- and $P(\delta_1^1)$-wave phase-shift solutions. The spectral functions so obtained can be used in calculations of the $\pi\pi$-system exchange contributions to the NN interaction. The implications of these spectral functions on nonrelativistic configuration-space generalized one-boson exchange potentials[2(a),2(b),2(e),2(f)] (GOBEP) for the NN interaction as well as on the corresponding relativistic momentum-space potentials for use with the Bethe-Salpeter equation[2(c)] are discussed.

Other studies and applications of finite-width corrections to the B_r propagator not cited in this paper previously have been made.[14-21] In Sec. VI we present a discrete N-pole approximation to our continuous spectral function, and this allows easy comparison with the one- and two-pole approximations of others. In the work of Furuichi *et al.*[14] spectral functions for scalar and vector bosons are presented, and the case of the ρ meson is analyzed explicitly. The conclusion was that "the width effect can be taken into account by the renormalization of coupling constants and the replacement of the observed mass by an effective one." This point of view is consistent with Scotti and Wong[6(c)] as both papers predict a lowering of m_ρ(eff) beneath m_ρ in their one-pole approximations. These results are analogous to our one-pole approximation for the ρ meson of Ref. 8 or Sec. VI; however, our fits to the δ_1^1 $\pi\pi$ phase shift predict a raising of this effective mass which we call $\bar{m}_\rho$. In Refs. 2(b), 6(d), 8, 19, and 20, two-pole representations of δ_0^0 (or the ϵ, σ, or S^* mesons) were used, where the lower-mass pole improves the fits to the NN phase shifts. Our two-pole approximation now fixes the positions of these poles and their relative coupling constants using the key moments of the spectral function.

II. RELATIVISTIC $\pi\pi$ RESONANCE RELATIONSHIPS

The general relationship between the FD expansion of the S matrix and the elastic scattering amplitude A is given by

$$\begin{aligned} S &= T\left\{\exp\left[-i\int \mathcal{H}_I(x)d^4x\right]\right\} \\ &= I + S_2 + S_4 + S_6 + \cdots \\ &= I + 2iA\,, \end{aligned} \tag{2.1}$$

where $S^\dagger S = I$ and

$$S_n = \frac{(-i)^n}{n!}\int d^4x_1 \cdots d^4x_n\, T[\mathcal{H}_I(x_1)\cdots\mathcal{H}_I(x_n)]\,. \tag{2.2}$$

After taking matrix elements and doing a partial-wave expansion we get

$$\begin{aligned} S_l(s) &= e^{2i\delta_l(s)} \\ &= 1 + S_{2l}(s) + S_{4l}(s) + \cdots \\ &= 1 + 2iA_l(s) \\ &= \left[\frac{1 + i\tan(\delta_l/\sigma)}{1 - i\tan(\delta_l/\sigma)}\right]^\sigma, \end{aligned} \tag{2.3}$$

$$\begin{aligned} A_l &= \sin\delta_l\, e^{i\delta_l} \\ &= (\cot\delta_l - i)^{-1} \\ &= \tfrac{1}{2}\sin 2\delta_l + i\sin^2\delta_l \end{aligned} \tag{2.4}$$

for the relationship between S_l, A_l, and δ_l, which is the phase shift of A_l. The unitarity condition $S_l^* S_l = 1$ allows one to express A_l in terms of only its phase. The last part of Eq. (2.3) holds for arbitrary real nonzero values of the parameter σ, and will be used later in discussion of unitarization schemes.

A. $\pi\pi$ amplitudes and phase shifts

Following the analyses of resonances of Jackson[12] and PR[13] a general BW amplitude can be written:

$$\begin{aligned} A_l(s) &= \frac{m_r\Gamma_l(s)}{s_r - s - im_r\Gamma_l(s)} \\ &= \frac{m_r(s_r - s)\Gamma_l(s) + is_r\Gamma_l^{\,2}(s)}{(s_r - s)^2 + s_r\Gamma_l^{\,2}(s)}, \end{aligned} \tag{2.5}$$

$$\Gamma_l(s) = \theta(s - a_r)\theta(b_r - s)\Gamma_r f_l(s), \tag{2.6}$$

$$f_l(s) = \left(\frac{s}{s_r}\right)^{n/2}\left(\frac{s - a_r}{s_r - a_r}\right)^{l+1/2}\frac{r_l(s)}{r_l(s_r)}, \tag{2.7}$$

where specific cases of the resonance shape function $f_l(s)$ are discussed for various values of n and functions $r_l(s)$. We show $\mathrm{Re}A_l$ and $\mathrm{Im}A_l$ for real s explicitly for later use. The functional dependence of A_l, Γ_l, and f_l on the resonance parameters of B_r (e.g., $m_r = s_r^{1/2}$, Γ_r, a_r, b_r) is suppressed when possible. Many works let $b_r \to \infty$; however, PR[13] used $b_r^{1/2} = \omega_c$ and Fulco, Shaw, and Wong[15] used $b_r^{1/2} = \Lambda$. Our use of b_r will allow us to generalize our amplitude to represent a sequence of nonoverlapping resonances on the same partial wave. The related problem of a system of overlapping resonances on the same partial wave has been examined by Coulter and Shaw.[22] The shape function $f_l(s)$ satisfies $f_l(a_r) = 0$, $f_l(s_r) = 1$,

and the threshold scattering-length relationship as $s \to a_r$ or $q^2 \to 0$ of

$$\tan\delta_l(s) = m_r\Gamma_l(s)/(s_r - s) \approx a_l q^{2l+1} = a_l[\tfrac{1}{4}(s-a_r)]^{l+1/2} \quad (2.8)$$

$$a_l = \frac{4^{l+1/2} m_r \Gamma_r}{(s_r - a_r)^{l+3/2}} \left(\frac{a_r}{s_r}\right)^{n/2} \frac{r_l(a_r)}{r_l(s_r)}, \quad (2.9)$$

where a_l is the scattering length. Equations (2.5)–(2.9) are essentially consistent with most resonance studies. This amplitude goes over to the nonrelativistic BW amplitude[13] if we identify $s = E^2$, $m_r = s_r^{1/2} = E_r$, and let $E \approx m_r$ in $(m_r + E)$, or

$$s_r - s = m_r^2 - E^2 = (m_r + E)(m_r - E) \approx 2m_r(m_r - E), \quad (2.10)$$

$$A_l(s) = A_l(E) \approx \frac{\frac{1}{2}\Gamma_l(E)}{E_r - E - i\frac{1}{2}\Gamma_l(E)}. \quad (2.11)$$

The amplitude also satisfies the two resonance conditions

$$\delta(E_r) = \tfrac{1}{2}\pi = \delta(s_r), \quad (2.12)$$

$$d\delta(E_r)/dE = 1/(\tfrac{1}{2}\Gamma_r) = 2m_r d\delta(s_r)/ds, \quad (2.13)$$

which define the resonance mass and width parameters in terms of phase behavior, where $ds(s_r)/dE = 2E_r = 2m_r$.

Our choice of $f_l(s)$ is the symmetric form

$$f_l(s) = \left[\left(\frac{s - a_r}{s_r - a_r}\right)\left(\frac{b_r - s}{b_r - s_r}\right)\right]^{l+1/2}, \quad (2.14)$$

since we will be giving b_r the interpretation of the position of the lower threshold of the next resonance on the same partial wave. This choice is similar to Eq. (36) of PR.[13] The resulting scattering length is

$$a_l = \frac{4^{l+1/2} m_r \Gamma_r}{(s_r - a_r)^{l+3/2}} \left(\frac{b_r - a_r}{b_r - s_r}\right)^{l+1/2}. \quad (2.15)$$

This form of $f_l(s)$ satisfies $f_l(b_r) = 0$, and $f_l(s) \to 1$ or $\Gamma_l(s) \to \Gamma_r$ as $a_r \to -\infty$ and $b_r \to +\infty$. The maximum of $f_l(s)$ occurs at $\frac{1}{2}(a_r + b_r)$, the midpoint of the range (a_r, b_r), and $f_l(s)$ is symmetric about this point. A fit of our amplitude to the phase-shift data directly is performed by using the imaginary part of Eq. (2.4) in the form

$$\delta_l(s) = \arcsin[\operatorname{Im} A_l(s)]^{1/2} \quad (2.16)$$

and varying (m_r, Γ_r) over the range of resonance data (a_r, b_r) to get the best fit. Our choice of $f_l(s)$ will allow us to fit highly skewed resonance phase-shift data, as we will illustrate with the S^* meson in Sec. V, as well as the more symmetric cases such as the ρ meson.

The range $(a_r^{1/2}, b_r^{1/2})$ for B_r with mass parameter m_r will be related in Sec. III to that range where the probability mass distribution for B_r is nonzero. Now r will be used to index a system of resonances on $\delta_l(s)$. The kinematic threshold of B_r may determine a_r, or (a_r, b_r) can be determined from experiment (e.g., phase shifts or cross sections). It will be assumed that the ranges (a_r, b_r) do not overlap, and that $b_r = a_{r+1}$. This can be viewed as the continuity requirement on $\delta_l(s)$ of $\delta_l(b_r) = \delta(a_{r+1})$. The extension of our amplitude to an amplitude representing a system of these resonances on $\delta_l(s)$ is given by

$$A_l(s) = \sum_r A_l(s, s_r, \Gamma_r, a_r, b_r), \quad (2.17)$$

where $A_l(s) = A_l(s, s_r, \Gamma_r, a_r, b_r)$ for $s \in (a_r, b_r)$. The phase shift of this generalized amplitude satisfies $\delta_l(a_r) = \delta_l(b_{r'}) = 0$ or π, $\delta_l(s_r) = \frac{1}{2}\pi$, and $d\delta_l(s_r)/ds = 1/(m_r\Gamma_r)$ for all (r, r') on $\delta_l(s)$. One could also choose to impose continuity requirements on $d\delta_l(s)/ds$ for $s = b_r = a_{r+1}$, though we chose not to in this paper. Now $A_l(s)$ can be fitted to each resonance section (a_r, b_r) of $\delta_l(s)$ between 0 and π to obtain that section's fit parameters (m_r, Γ_r). That section of the amplitude can then be searched for poles in the complex s plane, or equivalently the denominator

$$(s_r - s)^2 + s_r\Gamma_r^2\left[\left(\frac{s - a_r}{s_r - a_r}\right)\left(\frac{b_r - s}{b_r - s_r}\right)\right]^{2l+1} = 0 \quad (2.18)$$

can be searched for zeros. For $l = 0$ or δ_0^0 our quadratic denominator in s has two roots, and for $l = 1$ or δ_1^1 we can have six roots.

B. Unitarization and finite-width propagators

To relate our amplitude to the FD theory we could approximate A_l, and consequently S_l, by the Born amplitude

$$A_l(s) \approx B_l(s) = -\tfrac{1}{2}iS_{2l}(s), \quad S_l(s) \approx 1 + 2iB_l(s), \quad (2.19)$$

but this approximation is no longer unitary. One can now utilize K-matrix unitarization to improve the approximation where $K_l \approx K_{2l} = iS_{2l} = -2B_l$, and

$$S_l = \frac{1 - \frac{1}{2}iK_l}{1 + \frac{1}{2}iK_l} \approx \frac{1 - \frac{1}{2}iK_{2l}}{1 + \frac{1}{2}iK_{2l}} = \frac{1 + iB_l}{1 - iB_l}. \quad (2.20)$$

The general form for B_l is given by

$$B_l = g^2 h_l(s)\Delta(s, s_r), \quad (2.21)$$

where $s_r - i0$ is the pole of the singular part Δ of the propagator of the ϕ_i^B field of mass m_r given

by $P_{ij}=\Lambda_{ij}(p)\Delta(p^2,m_r^2)$. The spin part of the propagator Λ_{ij} [e.g., for spin $=l=1$; $\Lambda_{\mu\nu}=\delta_{\mu\nu}+(p_\mu p_\nu/m_r^2)$] and the form of the coupling [e.g., Γ_i in Eq. (1.6)] exactly determine $h_l(s)$.

A more general unitarization of $S\approx S(B)$ (temporarily suppressing the subscript l) is given by

$$S(B,\sigma)=\left[\frac{1+i(B/\sigma)}{1-i(B/\sigma)}\right]^{\sigma}, \tag{2.22}$$

where σ is a nonzero free parameter, and this satisfies

$$\begin{aligned} &S(-B,\sigma)=S^{-1}(B,\sigma)=S^*(B,\sigma),\\ &S(B,-\sigma)=S(B,\sigma),\\ &S(B,\sigma)=1+2iB+O(B^2). \end{aligned} \tag{2.23}$$

The last equation applies for small B, and relates $B=-\frac{1}{2}iS_2$. For the case $\sigma=1$ we have the K-matrix unitarization given by $S(B,1)$. In the limit $\sigma\to\infty$ we obtain an FD type of unitarization[2(g)]

$$\begin{aligned} S(B,\infty)&=e^{2iB}\\ &=e^{S_2}\\ &=\exp\left\{-\tfrac{1}{2}\int d^4x_1\,d^4x_2\,T[\mathcal{H}_I(x_1)\mathcal{H}_I(x_2)]\right\}, \end{aligned} \tag{2.24}$$

which illustrates the off-shell matrix aspect of $S(B,\sigma)$ if one replaces the matrix element B by the matrix $-\frac{1}{2}iS_2$. Each $S(S_2,\sigma)$ can be viewed as an expansion in powers of S_2 giving an approximation to the elastic FD expansion by

$$\begin{aligned} &S=1+S_2+S_4+S_6+\cdots\\ &\approx S(S_2,\sigma)=1+S_2+a_{\sigma 2}S_2^{\,2}+a_{\sigma 3}S_2^{\,3}+\cdots,\\ &S_{2n}\approx a_{\sigma n}S_2^{\,n}, \end{aligned} \tag{2.25}$$

where $a_{\sigma n}$ are determined by the choice of σ. Using Eq. (2.3) if

$$S=e^{2i\delta}\approx S(B,\sigma), \tag{2.26}$$

then the general relationship between B and δ is

$$B/\sigma=\tan(\delta/\sigma), \tag{2.27}$$

with the geometrical interpretation illustrated for arbitrary σ in Fig. 3. From the point of view of an expansion in B^n for $n=0$ we are at (1, 0) on the unitary circle, and $n=1$ takes us to (1, 2B) off the unitary circle. The addition of each term for $n=2, 3, 4, \ldots$ causes the eventual approach to $S=e^{2i\delta}$ on the unitary circle, where different choices of σ will effect the speed of approach to S depending on the size of B. For the limit $\sigma\to\infty$ we have the consistent result

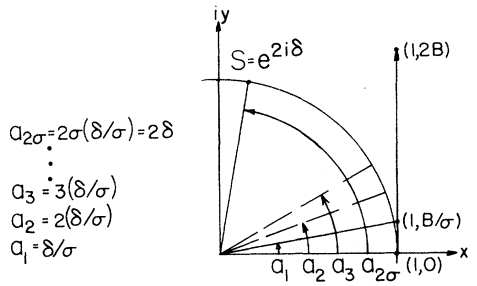

FIG. 3. Geometry of $S(B,\sigma)$ unitarizations.

$$\begin{aligned} &S=e^{2i\delta}\approx S(B,\infty)=e^{2iB},\\ &B=\lim_{\sigma\to\infty}[\sigma\tan(\delta/\sigma)]=\delta. \end{aligned} \tag{2.28}$$

Since $S(B,1)$ will yield a scattering amplitude which corresponds to the nonrelativistic Breit-Wigner resonant amplitude it will be used in this work.

The unitary approximation of S_l by Eqs. (2.20) and (2.21) can be viewed as an expansion in g^2 by expanding $(1-iB_l)^{-1}$, thereby yielding the diagrams of Fig. 2(b). Its effect is to distribute the pole at s_r-i0 yielding the finite-width unitarized Born amplitude

$$\begin{aligned} S_l&=\frac{1+ig^2h_l(s)/(s_r-s)}{1-ig^2h_l(s)/(s_r-s)}\\ &=\frac{s_r-s+ig^2h_l(s)}{s_r-s-ig^2h_l(s)}\\ &=1+2iB_{l\Gamma},\\ B_{l\Gamma}&=g^2h_l(s)\bar{\Delta}(s,g^2)\\ &=\frac{g^2h_l(s)}{s_r-s-ig^2h_l(s)}. \end{aligned} \tag{2.29}$$

Comparing B_l and $B_{l\Gamma}$ one could say that the unitarization changed the zero-width factor $\Delta(s,s_r)$ into $\bar{\Delta}(s,g^2)$ with finite width $m_r\Gamma_l(s)=g^2h_l(s)$. As $g^2\to+0$ we recover lowest-order perturbation theory, since $\bar{\Delta}(s,g^2)\to\Delta(s,s_r)$ and $B_{l\Gamma}/g^2\to B_l/g^2$. In relation to Fig. 2(c) we present two alternate interpretations. We can place a factor $g[h_l(s)]^{1/2}$ at each vertex and identify $\bar{\Delta}$ as the B_r propagator of the left-hand side of Fig. 2(b), where g will later be absorbed in g_{NNB_r} and $h_l(t)$ will modify the NNB_r form factor. Or we can identify the whole amplitude

$$B_{l\Gamma}(s)=\bar{\Delta}^{g}(s,g^2) \tag{2.30}$$

as the B_r propagator represented by the left-hand side of Fig. 2(b). The latter interpretation has the advantage of keeping $F(t)$ and $\bar{\Delta}^g$ as separate factors, or equivalently separating the analyses of Figs. 2(a) and 2(b). These two interpretations will

result in different spectral functions. It is useful to define the constants

$$I=\int_{-\infty}^{\infty}\mathrm{Im}\bar{\Delta}(s',\Gamma)ds',$$
$$I^{g}=\int_{-\infty}^{\infty}\mathrm{Im}\bar{\Delta}^{g}(s',\Gamma)ds', \tag{2.31}$$

as they will be used later to determine the normalization constants (N, N^g) which allow one to go to the normalized propagators

$$\Delta(s,\Gamma)=N\bar{\Delta}(s,\Gamma),\quad \Delta^{g}(s,\Gamma)=N^{g}\bar{\Delta}^{g}(s,\Gamma) \tag{2.32}$$

by applying a dispersion relation. We require a normalized propagator to satisfy Eqs. (1.7), (1.8), and (1.9).

Using this lowest-order perturbation theory as a guide we now identify finite-width propagators in our general amplitude of Eqs. (2.5) and (2.6):

$$A_I(s)=\bar{\Delta}^{g}(s,\Gamma)=m_r\Gamma_I(s)\bar{\Delta}(s,\Gamma), \tag{2.33}$$
$$\bar{\Delta}(s,\Gamma)=[s_r-s-im_r\Gamma_I(s)]^{-1}, \tag{2.34}$$

which are designed in Eq. (2.14) to allow a good fit to the full S matrix and corresponding phase-shift data. Now either $\bar{\Delta}(s,\Gamma)$ represents the left-hand side of Fig. 2(b) and $g_{NNB_r}F(t)[f_I(t)]^{1/2}$ appears at each vertex in Fig. 2(c), or $\bar{\Delta}^{g}(s,\Gamma)$ represents the left-hand side of Fig. 2(b) and $g_{NNB_r}F(t)$ appears at each vertex in Fig. 2(c). In Sec. VI we present the latter case. In both cases g_{NNB_r} is the renormalized NNB_r coupling constant including higher-order terms; e.g., $g_{NN\pi}{}^{2}g_{\pi\pi B_r}$ represented by the second diagram on the right-hand side of Fig. 2(a). Using our unitarized Born amplitude as a guide we assume $g_{\pi\pi B_r}{}^{2}\propto m_r\Gamma_r$, and for convenience we let $g^2=m_r\Gamma_r$ and suppress the subscript r when possible.

III. CORRESPONDING SPECTRAL FUNCTIONS AND MASS DISTRIBUTIONS

The standard dispersion relations[9] of $\bar{\Delta}$ and $\bar{\Delta}^{g}$ are

$$\bar{\Delta}(s,\Gamma)=\frac{1}{\pi}\int_{-\infty}^{\infty}\frac{\mathrm{Im}\bar{\Delta}(s',\Gamma)ds'}{s'-s-i0},$$
$$\bar{\Delta}^{g}(s,\Gamma)=\frac{1}{\pi}\int_{-\infty}^{\infty}\frac{\mathrm{Im}\bar{\Delta}^{g}(s',\Gamma)ds'}{s'-s-i0}. \tag{3.1}$$

These equations can be written as normalized distributions of the stable particle propagator, $\Delta(s,s')$, of Eq. (1.8) with a variable pole at $s'=m'^{2}$ by multiplying by

$$N=\pi/I,\quad N^{g}=\pi/I^{g} \tag{3.2}$$

to obtain normalized resonance or distributed mass propagators with finite width:

$$\Delta(s,\Gamma)=N\bar{\Delta}(s,\Gamma)=\int_{-\infty}^{\infty}\Delta(s,s')\rho(s')ds', \tag{3.3}$$
$$\Delta^{g}(s,\Gamma)=N^{g}\bar{\Delta}^{g}(s,\Gamma)=\int_{-\infty}^{\infty}\Delta(s,s')\rho^{g}(s')ds'. \tag{3.4}$$

Here $\rho(s')$ and $\rho^{g}(s')$ are our corresponding normalized spectral functions or mass-squared distributions satisfying

$$\rho(s')=I^{-1}\mathrm{Im}\bar{\Delta}(s',\Gamma)=\pi^{-1}\mathrm{Im}\Delta(s',\Gamma),$$
$$\rho^{g}(s')=(I^{g})^{-1}\mathrm{Im}\bar{\Delta}^{g}(s',\Gamma)=\pi^{-1}\mathrm{Im}\Delta^{g}(s',\Gamma),$$
$$\int_{-\infty}^{\infty}\rho(s')ds'=1=\int_{-\infty}^{\infty}\rho^{g}(s')ds', \tag{3.5}$$
$$\int_{-\infty}^{\infty}\mathrm{Im}\Delta(s',\Gamma)ds'=\pi=\int_{-\infty}^{\infty}\mathrm{Im}\Delta^{g}(s',\Gamma)ds'.$$

The probability interpretation is that

$$\rho(s')ds'=2m'\rho(m'^{2})dm'=\omega(m')dm' \tag{3.6}$$

is the probability that the pole s' of $\Delta(s,\Gamma)$ is in the range $(s', s'+ds')$, or that m'^{2} is in $(m'^{2}, m'^{2}+dm'^{2})$, or that m' is in $(m', m'+dm')$, where $\omega(m')=2m'\rho(m'^{2})$ is the mass distribution of $\Delta(s,\Gamma)$. Corresponding g equations also have the same interpretation.

The spectral functions for the two cases studied in this paper are obtained by using Eqs. (2.31)–(2.34) in Eq. (3.5). The values of the spectral functions at $s'=s_r$ can be used to conveniently relate these functions through the relationship between the imaginary parts of the propagators;

$$\rho(s_r)=(Ig^{2})^{-1},\quad \rho^{g}(s_r)=(I^{g})^{-1}$$
$$\mathrm{Im}\bar{\Delta}^{g}(s,\Gamma)=\rho^{g}(s)/\rho^{g}(s_r)$$
$$=m_r\Gamma_I(s)\,\mathrm{Im}\bar{\Delta}(s,\Gamma) \tag{3.7}$$
$$=f_I(s)\rho(s)/\rho(s_r).$$

We can now use Eqs. (2.16), (2.33), (2.34), and (3.7) to get a unique relationship between our spectral functions and the phase-shift data.

The relationship between the two interpretations can be clarified if one defines expectation values by

$$\langle h\rangle=\int_{-\infty}^{\infty}h(s')\rho(s')ds',$$
$$\langle h\rangle^{g}=\int_{-\infty}^{\infty}h(s')\rho^{g}(s')ds' \tag{3.8}$$

and notes that for most choices of $f_I(s)$ one has $\langle f\rangle\approx 1\approx\langle f\rangle^{g}$. The relationships between I and I^g, and between N and N^g are given by

$$I^g = Ig^2\langle f\rangle, \quad N^g = N/\langle f\rangle g^2, \quad \langle f\rangle = 1/\langle f^{-1}\rangle^g. \tag{3.9}$$

This leads to the general relationship

$$\rho^g(s') = [f_l(s')/\langle f\rangle]\rho(s'), \tag{3.10}$$

where $[f_l(s')/\langle f\rangle]$ acts as a weighting function on $\rho(s')$ yielding $\rho^g(s')$. To obtain a feeling for the values of I and I^g we look at the case $f_l(s')=1$ for $s'\in(-\infty,\infty)$ and obtain the familiar Breit-Wigner result

$$I = I^g/g^2 = g^2\int_{-\infty}^{\infty}\frac{ds'}{(s'-s_r)^2+g^4} = \pi. \tag{3.11}$$

A consistency check on $\rho(s')$ and $\rho^g(s')$ should be their approach to the δ function as $g^2\to 0$. Noting that the δ function satisfies

$$\delta(x-x_0) = \lim_{\epsilon\to+0}\frac{1}{\pi}\frac{\epsilon}{(x-x_0)^2+\epsilon^2},$$
$$\delta(s'-s_r) = \frac{\delta(m'-m_r)}{2m'}, \tag{3.12}$$

and that it is defined over $(-\infty,\infty)$, we first let $(a,b)\to(-\infty,\infty)$ to obtain the range of the δ function. This results in the constant-width BW or Cauchy distribution,

$$\rho^g(s') = \rho(s') = \frac{1}{\pi}\frac{g^2}{(s_r-s')^2+g^4}, \tag{3.13}$$

and finally as $g^2\to+0$ we obtain

$$\lim_{g^2\to+0}\rho(s') = \delta(s'-s_r) = \frac{\delta(m'-m_r)}{2m'} = \frac{1}{2m'}\lim_{g^2\to+0}\omega(m'). \tag{3.14}$$

The moments of $\rho^g(s')$ can be determined by

$$(T_n)^{-n} = \langle s'^{-n}\rangle^g, \quad \bar{m} = T^{1/2} = \langle s'^{1/2}\rangle^g, \tag{3.15}$$

where $\bar{m}$ is the mean mass. It is of interest to compare $m_{\max}$ defined by

$$d\rho^g(s_{\max})/ds' = 0, \quad s_{\max} = m^2{}_{\max}, \tag{3.16}$$

with $\bar{m}$, and we find in general that $m_{\max} = m_r$.

IV. THE INELASTIC CASE

If we introduce a real absorption parameter $\eta_l(s)$, which is equivalent to introducing an imaginary part to the phase shift, then

$$S_l = \eta_l e^{2i\delta_l}, \quad 0\le\eta_l\le 1$$
$$S_l^* S_l \le 1. \tag{4.1}$$

The modified propagator and spectral function can be obtained from

$$S_l = \eta_l e^{2i\delta_l} = 1 + 2i\bar{\Delta}^g(s,\Gamma) = \eta_l\left[\frac{s_r - s + im_r\Gamma_l(s)}{s_r - s - im_r\Gamma_l(s)}\right], \tag{4.2}$$

giving in terms of $n_\pm = \frac{1}{2}(1\pm\eta_l)$

$$\bar{\Delta}^g(s,\Gamma) = \frac{n_+ m_r\Gamma_l(s) + in_-(s_r-s)}{s_r - s - im_r\Gamma_l(s)},$$
$$\rho^g(s) = (I^g)^{-1}\,\mathrm{Im}\bar{\Delta}^g(s,\Gamma) = \frac{1}{I^g}\frac{[n_+ s_r\Gamma_l{}^2(s) + n_-(s_r-s)^2]}{(s_r-s)^2 + s_r\Gamma_l{}^2(s)}, \tag{4.3}$$

where $\rho^g(s_r) = n_+/I^g$. The introduction of the inelastic data is not further pursued in this paper.

V. APPLICATION TO THE $\pi\pi$ $S(\delta_0^0)$ AND $P(\delta_1^1)$ WAVES

We now fit our amplitude of Eq. (2.17) to the phase-shift data, where the fit of B_r over the (a_r, b_r) range of $\delta_l(s)$ determines $(m_r, \Gamma_r, a_r, b_r)$. These parameters along with a_l^I determined by Eq. (2.15), and key moments $(\bar{m} = T^{1/2}, T_1{}^{1/2}, T_2{}^{1/2})$ of ρ^g determined by Eqs. (3.15) using numerical integration are given in Table I, and the corresponding fits are shown in Fig. 4. The S-wave data follows the solutions given by the Particle Data Group of Baton *et al.*,[23] Carroll *et al.*,[24] and Flatté *et al.*,[25] and the P-wave solutions are by Baton *et al.*[23] and Scharenguivel *et al.*[26] as given in Moffat and Weisman.[27]

An interesting result is the very close relationship between the fits of the Baton *et al.* down solution denoted ϵd and the Flatté S^* solution. The reflection of the ϵd solution through $\frac{1}{2}\pi$, or the replacement of δ by $(\pi-\delta)$ for $\delta > \frac{1}{2}\pi$ as is shown by the dashed δ_0^0 curve of Fig. 4, is quite close to the S^*, and spectral functions which depend on $\sin^2\delta = \sin^2(\pi-\delta)$ can therefore hardly distinguish between the two cases. One could in fact omit introducing the ϵ altogether if the down solution below the S^* emerges as correct and just view this solution as the continuation of the S^* to its low-energy threshold. The recent work of Protopopescu *et al.*[28] supports this last point of view.

Since our values of (m,Γ) are determined by the behavior of the phase shift δ_0^0 and its first derivative at $\frac{1}{2}\pi$ [Eq. (2.13)], they are not to be compared with pole parameters. A search of our amplitude for poles, or its denominator [Eq. (2.18)] for zeroes, resulted in a $(718-i389)$-MeV pole for the somewhat symmetric ϵ solution. A search of the S^* solution's amplitude led to no pole, an acceptable situation recently discussed by Fonda, Ghirardi, and Shaw.[29] This is consistent with the S^* pole of Ref. 28 of $(997-i27)$ MeV since the asym-

TABLE I. Calculated meson parameters and corresponding data with r subscript suppressed.

			Data or parameters										
δ_l^I	Ref.	Meson	m (GeV)	Γ (GeV)	$a^{1/2}$ (GeV)	$b^{1/2}$ (GeV)	$T_1^{1/2}$ (GeV)	$T_2^{1/2}$ (GeV)	$\bar{m}=m_H=T^{1/2}$ (GeV)	P	$m_L=t_2^{1/2}$ (GeV)	$(1-P)$	a_l^I $(m_\pi^{-(2l+1)})$
δ_0^0	23	ϵ	0.720	0.200	0.2774	1.000	0.689	0.665	0.717	0.966	0.392	0.034	0.19
	23	ϵd	0.865	0.500	0.2774	1.000	0.718	0.668	0.773	0.947	0.388	0.053	0.42
	25	S^*	0.890	0.400	0.2774	1.000	0.738	0.690	0.789	0.952	0.396	0.048	0.34
	24		1.270	0.300	1.000	1.550	1.268	1.259	1.281	0.986	0.819	0.014	0.29
δ_1^1	23	ρ	0.765	0.135	0.2774	1.300	0.786	0.774	0.803	0.970	0.506	0.030	0.021
	26	ρ	0.765	0.135	0.2774	1.600	0.823	0.805	0.857	0.940	0.553	0.060	0.017
	27	ϵ											0.19
		ρ											0.028
	30	S^*											0.15
		ρ											0.036

metry of this solution forced our pole in this direction onto the real axis at 1060 MeV, where $\theta(b_r - s)$ causes our S^* amplitude to vanish.

Two values of $b_\rho^{1/2}$ are given, depending on which of the high-energy data points one tries to fit, where the $b_\rho^{1/2}=1.6$ GeV dashed curve is consistently lower than the $b_\rho^{1/2}=1.3$ GeV curve except where they are equal at $m=0.765$ GeV. When Eq. (36) of PR[13] was used, a range for $b_\rho^{1/2}=\omega_c$ of 1.2 to 1.4 GeV resulted, as reported in their Table II.

The skewness of the spectral functions is reflected in the displacement of the key moment of ρ^s, $\bar{m}$, either above or below m. As $\bar{m}$ indicates a dominant input into the NN interaction of the $\pi\pi$ phase shifts (see Sec. VI), a close determination of the resonance parameters (m, Γ, a, b) becomes essential, as is indicated by the 54-MeV change in $\bar{m}_\rho$ obtained by changing only $b_\rho^{1/2}$ by 300 MeV.

The values of a_l^I can be compared with recent calculated values of Ref. 27 and Pennington and Protopopescu[30] listed in Table I. Since Ref. 27 only fits the Baton *et al.* up solution denoted ϵ, our value of a_0^0 only agrees for the fit of the spectral function to the ϵ data of δ_0^0. As a test case for comparison with a_0^0 of Refs. 27 and 30 we only changed Γ of the S^* parameters from 0.400 to 0.200 GeV, giving $a_0^0=0.17$; however, this resulted in too low (high) a fit to the S^* data below (above) $m=0.890$ GeV. A similar test case where only $b_\rho^{1/2}$ of the ρ parameters was changed to 1.120 GeV gave $a_1^1=0.028$, and resulted in a good (bad) fit to the δ_1^1 high-energy data of Ref. 26 (23) and a good fit to the remaining low-energy data.

VI. APPLICATION TO THE NN INTERACTION

Our configuration-space OBEP used in a nonrelativistic Schrödinger-equation calculation is given by[2(b)]

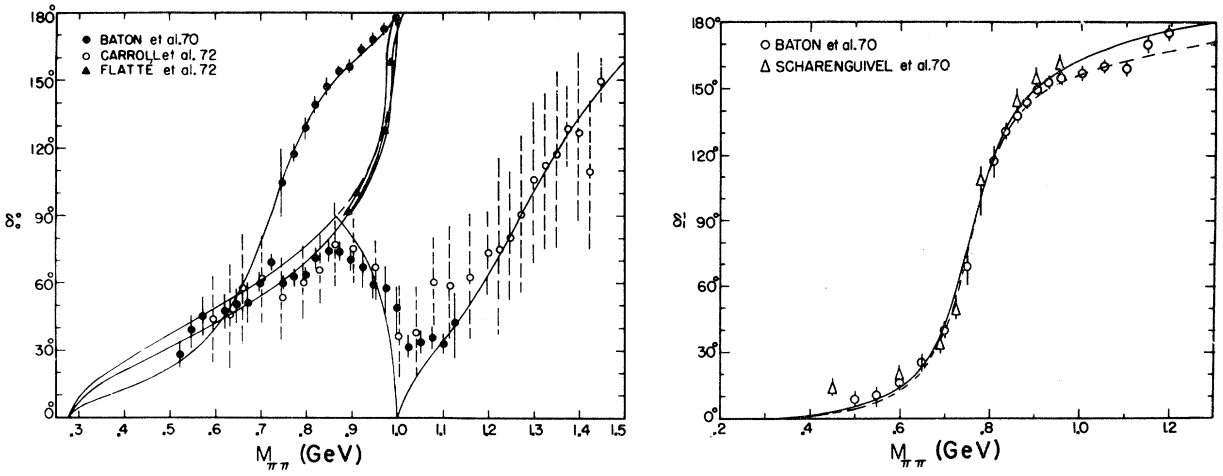

FIG. 4. Data and theoretical fits of the $\pi\pi$ δ_0^0 and δ_1^1 phase shifts.

$$Y^N(r,\Lambda,m_B)=\frac{1}{2\pi^2}\int d^3k\, e^{i\vec{k}\cdot\vec{r}}F^N(t,t_\Lambda)\Delta(t,t_B), \tag{6.1}$$

where $t_\Lambda=\Lambda^2$ is chosen to maximize the fit to the NN data, $t_B=m_B{}^2$, and $t=-\vec{k}^2$. The integrand

$$V^N(t,t_\Lambda,t_B)=F^N(t,t_\Lambda)\Delta(t,t_B) \tag{6.2}$$

gives the on-the-mass-shell momentum-space OBEP later used by Gersten, Thompson, and Green[2(c)] in a relativistic Bethe-Salpeter equation calculation. We now assume that our $\pi\pi$ s-channel results of Secs. II and III in the form of Eq. (3.4) can be applied in the form

$$\Delta(t,\Gamma)=\int_a^b \Delta(t,t')\rho^g(t')dt' \tag{6.3}$$

to give a more precise representation of the contribution of the $\pi\pi$ δ_0^0 and δ_1^1 phase shifts in the t channel of the NN interaction. The distributed mass potentials resulting from the use of Eq. (6.3) are

$$\begin{aligned} U^N(t,t_\Lambda)&=\int_a^b V^N(t,t_\Lambda,t')\rho^g(t')dt' \\ &=F^N(t,t_\Lambda)\Delta(t,\Gamma), \\ J^N(r,\Lambda)&=\int_a^b Y^N(r,\Lambda,t')\rho^g(t')dt' \\ &=\frac{1}{2\pi^2}\int d^3k\, e^{i\vec{k}\cdot\vec{r}}F^N(t,t_\Lambda)\Delta(t,\Gamma), \end{aligned} \tag{6.4}$$

where $t'=m'^2$. In our work we have predominantly used the quadrupole ($N=4$) regulated potential of Ueda and Green[2(b),2(e),2(f)]

$$Y^4(r,\Lambda,m)=\frac{1}{r\tau^4}\{e^{-mr}-e^{-\Lambda r}[1+\tfrac{1}{2}\Lambda r\tau+\tfrac{1}{8}\Lambda r(1+\Lambda r)\tau^2+\tfrac{1}{48}\Lambda r(3+3\Lambda r+\Lambda^2r^2)\tau^3]\}, \tag{6.5}$$

where $\tau=1-(m/\Lambda)^2$, which is equivalent to using a dipole nucleon-meson form factor, or the same order form factor used to fit the proton electromagnetic data.

Owing to the close relationship between the ϵd and S^* solutions discussed in Sec. V, the main implications of the differing $\pi\pi$ δ_0^0 solutions on the NN problem can be illustrated by comparing the ϵ and S^* solutions, and this can be seen in Fig. 5 by examining a coordinate-space difference function of the two potentials

$$D_{\epsilon S^*}=g_\epsilon{}^2J_\epsilon{}^4-g_{S^*}{}^2J_{S^*}{}^4. \tag{6.6}$$

To show this realistically we take $g_\epsilon{}^2=14$ and adjust $g_{S^*}{}^2$ so that the difference vanishes at 1 F. Such a cancellation brings the difference into the same order of magnitude as the residual static terms in current OBEP which survives after the major cancellation between the static repulsive contributions of the ω meson and the $\pi\pi$ static attractive contribution of the scalar isoscalar meson, i.e., the ϵ or S^*. It is the scalar-vector cancellation which makes the NN interaction so complicated not only by bringing out relativistic spin- and velocity-dependent terms which survive the cancellation, but also by amplifying the influence of the width and shape of the $\pi\pi$ phase shifts. The large difference function in the range (0, 1 F) indicates that the details of the $\pi\pi$ δ_0^0 phase shift significantly influence the character of the NN interaction in the core region. This difference can be partially compensated by the choice of Λ. For $r>1$ F the solid curve shows that the close agreement of this paper's ϵ and S^* phase-shift solutions in ($2m_\pi$, 0.66 GeV) results in similar long-range ($r>1$ F) potentials, thereby eliminating this part of the ambiguity between using the ϵ or S^* in the NN interaction. The dashed curve compares this

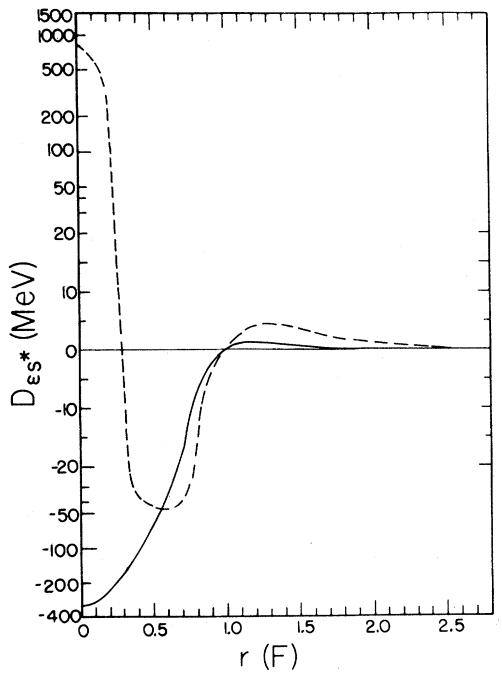

FIG. 5. $D_{\epsilon S^*}(r)$ in MeV for $\Lambda=2m_p=1877.8$ MeV, $g_\epsilon{}^2=14.0\hbar c$ MeV F, and $g_{S^*}{}^2$ is chosen so that $D_{\epsilon S^*}(1\text{ F})=0$. Our $\rho^g(t')$ is used for the S^*, and the solid (dashed) curve uses the distribution of $\rho^g(t')$ (Ref. 2(f)) for the ϵ. The vertical axis is linear in (−20, 20) and logarithmic in (20, 1500) and (−20, −400) MeV.

paper's distributed S^* with the sharply distributed ϵ of Ref. 2(f), where $\delta_0^0 \approx 0$ for $M_{\pi\pi} \leq 0.54$ GeV, and here the disparity in the phase-shift solutions in ($2m_\pi$, 0.66 GeV) is illustrated by the long-range (1, 2.4 F) values of the difference function.

The integrations over t' to calculate our distributed propagators [Eq. (6.3)] and potentials [Eq. (6.4)] as well as the moments of ρ^g [Eq. (3.15)] are performed using standard numerical techniques (e.g., Simpson's rule),

$$\langle f(t')\rangle^g = \int f(t')\rho^g(t')dt' \approx \sum_{i=1}^{N} W_i f(t_i)\rho^g(t_i), \tag{6.7}$$

and stability (independence of N) is achieved by brute force increase of N. This can be reexpressed by approximating our continuous mass-squared distribution by a discrete distribution or spectrum

$$\rho^g(t') \approx \sum_{i=1}^{N} P_i \delta(t' - t_i), \qquad \int f(t')\rho^g(t')dt' \approx \sum_{i=1}^{N} P_i f(t_i) = \langle f(t')\rangle^d, \tag{6.8}$$

where $P_i = W_i\rho^g(t_i)$ is the probability of t' being t_i, and the last equation defines discrete expectation values. No discretion has yet been used in selecting the $2N$ parameters (P_i, t_i) other than the choice of a particular method of numerical integration. However, we can hope for good accuracy at small N by imposing $2N$ conditions dependent on the key moments of ρ^g upon our discrete distribution as a means of selecting (P_i, t_i). The first condition is to equate zeroth moments, which fixes the normalizations:

$$\langle t'^0\rangle^g = 1 = \langle t'^0\rangle^d = \sum_{i=1}^{N} P_i . \tag{6.9}$$

For the case $f(t') = \Delta(t, t')$ this condition is equivalent to requiring our approximate propagator

$$\Delta(t, \Gamma) \approx \Delta^a(t, \Gamma) = \sum_{i=1}^{N} P_i \Delta(t, t_i) \tag{6.10}$$

to be equal to $\Delta(t, \Gamma)$ as $\vec{k}^2 \to \infty$.

For the case $N = 2$ we have $P_1 = P$ and $P_2 = 1 - P$, and we obtain good accuracy by also requiring $t_1 = T$ of Eq. (3.15) and equating two moments:

$$(T_1)^{-1} = \langle t'^{-1}\rangle^d = PT^{-1} + (1-P)t_2^{-1}, \qquad (T_2)^{-2} = \langle t'^{-2}\rangle^d = PT^{-2} + (1-P)t_2^{-2}. \tag{6.11}$$

These four conditions determine P and t_2 to be

$$P = \frac{1 - (t_2/T_2)^2}{1 - (t_2/T)^2}, \qquad t_2 = \frac{(T^2 - T_2^2)T_1 - [(T^2 - T_2^2)^2 T_1^2 - 4(TT_1 - T_2^2)(T - T_1)TT_2^2]^{1/2}}{2(TT_1 - T_2^2)} . \tag{6.12}$$

Equating moments for $n = 1, 2$ is equivalent to requiring $\Delta^a(t, \Gamma)$ and its first derivative to be equal to those values of $\Delta(t, \Gamma)$ at $\vec{k}^2 = 0$, and consequently this selection of (P_i, T_i) is similar to doing a Maclaurin expansion of $\Delta(t, \Gamma)$ and keeping lower-order terms. A similar approximation due to Gersten was used in Refs. 19 and 20; however, that approximation yielded unphysical parameters and made no use of $\bar{m}$, the key moment of the continuous distribution. The discrete parameters of our approximation, $\bar{m} = T^{1/2}$, P, $m_L = t_2^{1/2}$, and $(1 - P)$, are determined by Eqs. (6.11) and (6.12), and are given in Table I.

A simple physical interpretation is that P is the dominant probability that the resonance mass assumes the heavy value $m_H = \bar{m}$, and $(1 - P)$ is the smaller probability, reflecting the low-mass contribution of the continuous spectral function, that the resonance mass assumes the lighter value m_L. From this point of view, preceding works [e.g., Ref. 2(b)] which used real heavy scalar bosons and fictitious lighter scalar bosons in NN OBEP calculations with three free parameters (g_H^2, g_L^2, m_L) now have two of those parameters fixed; m_L and $g_L^2 = [(1-P)/P]g_H^2$.

The values of the approximation parameters for ϵ, ϵd and S^* of Table I show that $\bar{m}$ does dominate the discrete distribution ($P \geq 0.94$) and its spread of values over 72 MeV reflects the different heavy-mass contributions. However, the low-mass contributions are all quite similar with a spread of values of m_L over only 8 MeV, and this is an important contribution to the NN problem.

The approximate propagators and potentials are

$$\Delta^a(t, \Gamma) = P\Delta(t, \bar{m}^2) + (1-P)\Delta(t, m_L^2), \qquad J^{4a}(r, \Lambda) = PY^4(r, \Lambda, \bar{m}) + (1-P)Y^4(r, \Lambda, m_L). \tag{6.13}$$

In making comparisons for the ρ (using $b_\rho^{1/2} = 1.6$ GeV) and S^* mesons we find that the maximum % difference between $\Delta(t, \Gamma)$ and $\Delta^a(t, \Gamma)$ for $\vec{k}^2$ in

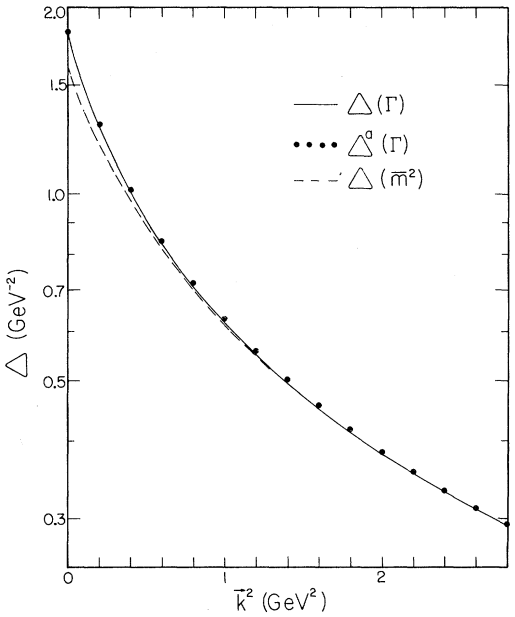

FIG. 6. The S^* propagators $\Delta(t, \Gamma)$ of Eq. (6.3), $\Delta^a(t, \Gamma)$ of Eqs. (6.13), and $\Delta(t, \bar{m}^2)$ of Eq. (1.8).

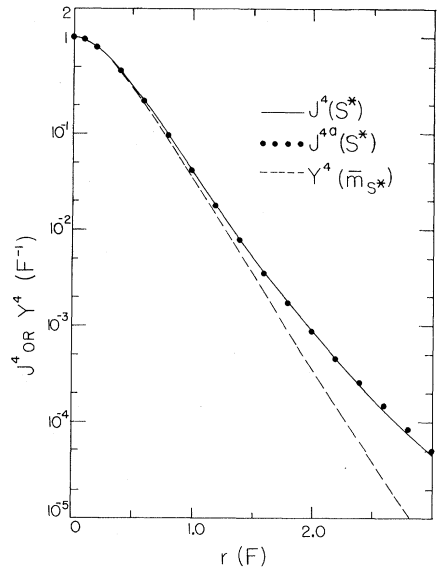

FIG. 7. The S^* potentials J^4 of Eq. (6.4), J^{4a} of Eq. (6.13), and $Y^4(r, \Lambda, \bar{m})$ of Eq. (6.5) for $\Lambda = 2m_\rho$.

0 (2) GeV^2 is 1.04 (1.41)% occurring at $\vec{k}^2 = 1.4$ (0.8) GeV^2 for the ρ (S^*). The maximum % difference between J^4 and J^{4a} for r in 0 (2) F is 2.2 (4.1)% occurring at $r = 1.6$ (1.8) F for the ρ (S^*). For increased accuracy one could choose (P_3, t_3) by equating values of our full and approximate functions at these points $(r, \vec{k}^2)$ of maximum % difference. In Fig. 6 we show for the S^* the distributed propagator $\Delta(t, \Gamma)$ of Eq. (6.3) (solid line), its two-pole approximation $\Delta^a(t, \Gamma)$ of Eq. (6.13) (dots), and a one-pole approximation $\Delta(t, \bar{m}^2)$ of Eq. (1.8) using $m^2 = \bar{m}^2$ (dashed line). The corresponding coordinate-space curves are shown in Fig. 7 for $\Lambda = 2m_\rho$, and we note that the approximation scheme uncouples the NN parameter Λ from the $\pi\pi$ phase-shift parameters of $\rho^s(t')$ or (P_i, t_i) of Eq. (6.10). In these figures we see the rapid convergence of the approximation scheme of this section, and also that the neglect of the low-mass components of δ_0^0 leads to incorrect values of our propagators (potentials) at small t (large r) in k (x) space.

VII. CONCLUSION

It was noted several years ago[2(e)] that NN phase-shift data, when interpreted with a GOBEP model, favors a broad resonance ($\gtrsim$300 MeV) in the high-mass ($\gtrsim$700 MeV) neighborhood, in contrast to a sharp ϵ resonance which was seriously considered at that time. In terms of currently accepted alternatives our past work reflects a compatability with the S^* or the ϵd solutions. With the more precise way of representing alternative $\pi\pi$ phase-shift solutions presented here, we believe we can explore with much greater precision the consequence of the $\pi\pi$ phase shifts upon the NN problem in both coordinate space using a nonrelativistic GOBEP formalism, and in momentum space using a relativistic GOBEP formalism.

ACKNOWLEDGMENTS

The authors would like to thank Dr. M. Parkinson for helpful conversations. Computer support from the North East Regional Data Center of the University of Florida is gratefully acknowledged.

*Present address: Computer Sciences Corporation, 8728 Colesville Road, Silver Spring, Maryland 20910.
†Now at Osaka University, Osaka, Japan.

[1]S. Sawada, T. Ueda, W. Watari, and M. Yonezawa, Prog. Theor. Phys. 28, 991 (1962); 32, 380 (1964).
[2](a) A. E. S. Green and T. Sawada, Nucl. Phys. B2, 276 (1967); Rev. Mod. Phys. 39, 594 (1967). (b) T. Ueda and A. E. S. Green, Phys. Rev. 174, 1304 (1968); Nucl. Phys. B10, 289 (1969). (c) A. Gersten, R. H. Thompson, and A. E. S. Green, Phys. Rev. D 3, 2076 (1971). (d) T. Ueda, Prog. Theor. Phys. 45, 1527 (1971). (e) R. W. Stagat, F. Riewe and A. E. S. Green, Phys. Rev. Lett. 24, 631 (1970); Phys. Rev. C 3, 552 (1971). (f) A. E. S. Green, F. Riewe, M. L. Nack, and L. D.

Miller, in proceedings of the Symposium on Present Status and Novel Developments in the Nuclear Many-Body Problem, Rome, 1972 (unpublished). (g) T. Inagaki, Prog. Theor. Phys. 48, 868 (1972).
[3]S. N. Gupta, Phys. Rev. 117, 1146 (1960); C. W. Bock and R. D. Haracz, Phys. Rev. D 5, 39 (1972); 6, 1373 (1972).
[4]M. Kikugawa, S. Sawada, T. Ueda, W. Watari, and M. Yonezawa, Prog. Theor. Phys. 37, 88 (1967).
[5]T. Ueda, in proceedings of the Symposium on Present Status and Novel Developments in the Nuclear Many-Body Problem, Rome, 1972 (unpublished); Prog. Theor. Phys. 48, 2276 (1972).
[6](a) A. Scotti and D. Y. Wong, Phys. Rev. 138, B145 (1965); (b) J. S. Ball, A. Scotti, and D. Y. Wong, *ibid.* 142, 1000 (1966); (c) D. Y. Wong, Rev. Mod. Phys. 39, 622 (1967); (d) K. S. Stowe and D. Y. Wong, Nuovo Cimento 18A, 427 (1973).
[7]M. Chemtob, J. W. Durso, and D. O. Riska, Nucl. Phys. B38, 141 (1972).
[8]T. Ueda, M. L. Nack, and A. E. S. Green, Phys. Rev. C 8, 2061 (1973).
[9]S. S. Schweber, *An Introduction to Relativistic Quantum Field Theory* (Harper and Row, New York, 1962); see Sec. 17b.
[10]A. E. S. Green, Phys. Rev. 75, 1926 (1948).
[11]M. L. Nack, T. Ueda, and A. E. S. Green, in π-π *Scattering—1973*, proceedings of the international conference on π-π scattering and associated topics, Tallahassee, 1973, edited by P. K. Williams and V. Hagopian (A.I.P., New York, 1973), p. 332.
[12]J. D. Jackson, Nuovo Cimento 34, 1644 (1964).
[13]J. Pišút and M. Roos, Nucl. Phys. B6, 325 (1968).
[14]S. Furuichi, S. Sawada, T. Ueda, W. Watari, and M. Yonezawa, Prog. Theor. Phys. 32, 966 (1964).
[15]J. R. Fulco, G. L. Shaw, and D. Y. Wong, Phys. Rev. 137, B1242 (1965).
[16]H. Pilkuhn, *The Interaction of Hadrons* (Wiley, New York, 1967).
[17](a) G. J. Gounaris and J. J. Sakurai, Phys. Rev. Lett. 21, 244 (1968). (b) G. L. Gounaris, Phys. Rev. 181, 2066 (1969).
[18]J. L. Petersen, Phys. Rep. 2C, 155 (1971).
[19]J. Binstock and R. Bryan, Phys. Rev. D 4, 1341 (1971).
[20]R. Bryan and A. Gersten, Phys. Rev. D 6, 341 (1972).
[21]F. Partovi and E. Lomon, Phys. Rev. D 5, 1192 (1972).
[22]P. W. Coulter and G. L. Shaw, Phys. Rev. D 8, 2216 (1973).
[23]J. P. Baton, G. Laurens, and J. Reignier, Phys. Lett. 33B, 525 (1970); 33B, 528 (1970).
[24]J. T. Carroll *et al.*, Phys. Rev. Lett. 28, 318 (1972).
[25]S. M. Flatté *et al.*, Phys. Lett. 38B, 232 (1972).
[26]J. Scharenguivel *et al.*, Purdue Univ. report, 1970 (unpublished).
[27]J. W. Moffat and B. Weisman, Phys. Rev. D 6, 238 (1972).
[28]S. D. Protopopescu *et al.*, Phys. Rev. D 7, 1279 (1973).
[29]L. Fonda, G. C. Ghirardi, and G. L. Shaw, Phys. Rev. D 8, 353 (1973).
[30]M. R. Pennington and S. D. Protopopescu, Phys. Rev. D 7, 1429 (1973).